

Robust Controller Design for Speed Regulation of a Wind Turbine using 16-Plant Theorem Approach

N. V. A. Ravikumar^{1,*}, G. Saraswathi²

¹Research Scholar, Department of Electrical & Electronics Engineering, JNTUK, Kakinada, Andhra Pradesh, India

¹Sr. Assistant Professor, Department of Power Engineering, GMR Institute of Technology, Rajam - 532127, Srikakulam, Andhra Pradesh, India

²Professor & Principal, University College of Engineering, Vizianagaram, JNTUK, Kakinada, Dwarapudi(post), 535003, Andhra Pradesh, India

Abstract

Large scale wind turbines are subjected to fatigue, aerodynamics, structural flexibility and wind turbulence which lead to uncertain behavior of the wind turbine. The uncertainties are due to differences between the mathematical model and the actual dynamics of the system in operation and the worn and torn effects. These elements are combinations of mass, stiffness, damping factors and moments of inertia of the rotor and generator. The uncertainties or perturbations in the wind turbine are indicated by variations between $\pm 25\%$ of the nominal values of the elements of the system matrix. These uncertainties in the wind turbine are dealt with the proposed robustly stabilizing controller in this paper. The stable (K_p, K_i) regions of a Proportional-Integral (PI) controller are chosen by the Kharitonov's theorem based 16-plant model. It can be shown that a simple PI controller can become robust by the correct selection of its parameters. The furnished results validate the above statement.

Received on 28 May 2019; accepted on 15 October 2018; published on 16 October 2019

Keywords: Robust control, Kharitonov's theorem, 16-plant theorem, PI controller, interval polynomial, interval plant

Copyright © 2019 N. V. A. Ravikumar, licensed to EAI. This is an open access article distributed under the terms of the Creative Commons Attribution license (<http://creativecommons.org/licenses/by/3.0/>), which permits unlimited use, distribution and reproduction in any medium so long as the original work is properly cited.

doi:10.4108/eai.16-10-2019.160841

1. Introduction

The present scenario in the world of energy experiences a rapid growth in wind energy that challenges the research interests of the systems and control domain. Various researchers have contributed in the field of wind turbine control. The description on the basic structure of wind turbines, the control loops and the controllers, [1], elaborates on the blade pitch control system. Additionally, the recent developments in the design of advanced controllers for wind turbines and wind farms were described. In [2], the statistical data is presented which clearly indicates that the overall installed capacity of wind power worldwide increased from 296,581 MW in the year 2013 to 539,291 MW by the end of year 2017. It was announced by World Wind Energy Association on 25 February 2019, that the overall capacity of all wind turbines installed

worldwide by the end of 2018 reached 600 Gigawatt. According to preliminary statistics, 53,900 Megawatt were added in the year 2018, slightly more than in 2017 when 52,552 Megawatt were installed. 2018 was the second year in a row with growing number of new installations but at a lower rate of 9.8%, after 10.8% growth in 2017. All wind turbines installed by end of 2018 can cover close to 6% of the global electricity demand.

This large wind power capture obviously leads to usage of large wind turbines. Large turbines have high specifications and a particular modern wind turbine may be designed to generate several MWs. The large wind turbines come with high cost, requires good maintenance, should withstand extreme weather conditions, mainly wind speed variations. The need for control of a wind turbine arises in medium and high wind speeds. Wind turbines are available as vertical-axis (VAWT) and horizontal-axis wind turbines (HAWT). Due to the evident advantages of HAWT over

*Corresponding author. Email: ravikumar.nva@gmrit.edu.in

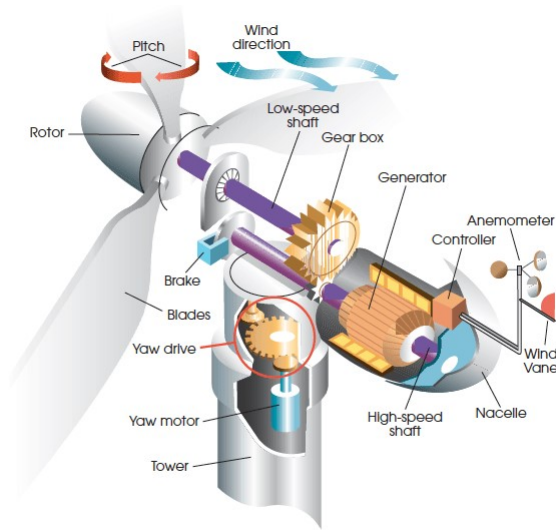


Figure 1. A Horizontal Axis Wind Turbine - components [4]

VAWT as mentioned in [1; 3] the HAWT machine is considered for study in this paper. Figure 1 shows the components of the up-wind HAWT machine as taken from [4]. The design of pitch control for variable speed wind turbine is reviewed in [5]. The pitch control primarily limits power in high winds.

In [6], the authors dealt with individual pitch control to limit power in high winds, particularly for large turbines. In [7], a power system stabilizer is proposed that is designed according to Kharitonov's extremal gain margin theory in a simulated environment. It stabilizes simultaneously limited number of extreme plants, and the resulting controller is a low-order phase-lead compensator, which is robust to the change of operating points. The design of PI controller to stabilize an interval plant family is discussed in [8], wherein a complete characterization of all stabilizing PI controller for an interval plant family is obtained. In [9], a robust controller is designed for an uncertain model that shows the design of H_∞ controller, μ -controller and loop shaping controller. The robust control under parametric uncertainty is overviewed in [10].

The potential threat to the stability and performance under the influence of uncertainties on the wind turbines gained prominence and is hence considered for analysis in this paper. The Kharitonov based design of PI controller [11] is a prominent design method, that specifically models a 16-plant model from the given interval plant. An acceptable stabilizing region for K_p and K_i values along with its Kharitonov rectangles are formulated using this method. A better insight into Kharitonov based controller is provided by various researchers in [12], about the 16-plant theorem in [13], the design of robust PID controllers in [14], [15], [16], [17] and [18].

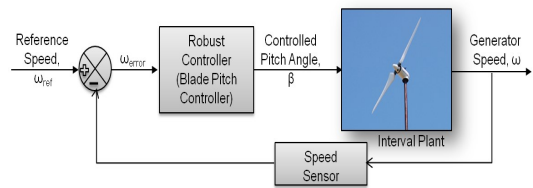


Figure 2. Feedback control of interval plant $p(s, a, b)$

Improper control of wind turbines subjected to uncertainties owing to its large size and cost may lead to loss in reliability and economic aspects. Therefore, the focus lays generally on the active control of larger flexible wind turbines subjected to uncertainties, that lead to reduction in the losses incurred economically and structurally which sums up to costly compensation which are quoted in [19]. The point of interest lies in the design of a controller for an uncertain wind turbine under the Kharitonov's polynomial environment to regulate the generator speed via the control of blade pitch angle β .

In [20], an uncertainty to the range of $\pm 20\%$ is applied on the same wind turbine that is considered for study in this paper. This $\pm 20\%$ uncertainty is applied on 15 elements of its system matrix with size 7×7 and a robust \mathcal{H}_∞ -controller is designed for speed regulation of an uncertain wind turbine. In this paper, it is found that when the uncertainty is applied on 13 elements of the system matrix, the range of uncertainty is increased to $\pm 25\%$. A robustly stabilizing K_p and K_i values of a Proportional-Integral controller is proposed for design of a 16-plant model based on the Kharitonov's theorem.

This paper is organized as follows: The introduction to an uncertain wind turbine and control methodologies were discussed in section 1. Section 2 discusses the linearized uncertain wind turbine CART2 model, section 3 covers the modelling of uncertain wind turbine while section 4 shows insights into the basics of Kharitonov's theorem. Section 5 shows the robust controller design using the 16-plant model while section 6 furnishes the simulation results for various scenarios encountered by the uncertain wind turbine model. Finally the conclusions are made from the obtained results for different uncertainties with the Kharitonov's rectangles, K_p and K_i acceptable stabilizing regions and the control of generator speed.

2. A Linearized Uncertain Modelling of the CART2 Wind Turbine

A Controls Advanced Research Turbine (CART2) developed in the National Wind Technology Center (NWTC), a sub-centre of National Renewable Energy Laboratory [21], Colorado is considered for study in this paper. The CART2 is a 600 kW, 2-bladed horizontal

axis wind turbine having the rotor collective blade pitch angle as the control input and the measured output variable is the generator speed. In [21; 22], there are reliable models of 1-state, 3-states, 5-states, 7-states and 9-states which consider the flexible bodies (blades, low speed shaft and tower) and the rigid bodies (earth, base plate, nacelle, generator and hub) of the wind turbine. Upon inclusion of $\pm 25\%$ uncertainty for the study in this paper the controllability and the observability of the uncertain wind turbine were preserved. Hence, in this paper, a robust controller is proposed to design for an uncertain 7-state interval model of the wind turbine. The block diagram of an uncertain interval plant model of the wind turbine and the robust controller is shown in Figure 2.

2.1. A Seven-State Linear Wind Turbine Model

The state space linearized model of a wind turbine with 7 states, a control input (u) and the measured control output (y) is expressed as

$$\begin{aligned} M\dot{x}(t) &= Ax(t) + Bu(t) \\ y(t) &= Cx(t) \end{aligned} \quad (1)$$

$$\begin{bmatrix} 1 & 1 & 0 & 0 & 0 & 0 & 0 \\ 0 & M_{11} & M_{14} & 0 & 0 & 0 & M_{17} \\ 0 & 2M_{14} & I_{rot} & 0 & 0 & 0 & 0 \\ 0 & 0 & 0 & 1 & 0 & 0 & 0 \\ 0 & 0 & 0 & 0 & I_{gen} & 0 & 0 \\ 0 & 0 & 0 & 0 & 0 & 1 & 0 \\ 0 & 2M_{71} & 0 & 0 & 0 & 0 & M_{77} \end{bmatrix} \begin{bmatrix} \dot{x}_1 \\ \dot{x}_2 \\ \dot{x}_3 \\ \dot{x}_4 \\ \dot{x}_5 \\ \dot{x}_6 \\ \dot{x}_7 \end{bmatrix} = \begin{bmatrix} 0 & 1 & 0 & 0 & 0 & 0 & 0 \\ -K_{11} & -C_{11} & -C_{14} & 0 & 0 & -K_{17} & -C_{17} \\ -2K_{41} & -2C_{41} & \gamma - C_d & -1 & C_d & -K_{47} & -C_{47} \\ 0 & 0 & K_d & 0 & -K_d & 0 & 0 \\ 0 & 0 & C_d & 1 & -C_d & 0 & 0 \\ 0 & 0 & 0 & 0 & 0 & 0 & 1 \\ -2K_{71} & -2C_{71} & -C_{74} & 0 & 0 & -K_{77} & -C_{77} \end{bmatrix} \begin{bmatrix} x_1 \\ x_2 \\ x_3 \\ x_4 \\ x_5 \\ x_6 \\ x_7 \end{bmatrix} + \begin{bmatrix} 0 \\ \zeta_b \\ \zeta \\ 0 \\ 0 \\ 0 \\ \zeta_t \end{bmatrix} \beta \quad (2)$$

$$y = [0 \ 0 \ 0 \ 0 \ 1 \ 0 \ 0] [x_1 \ x_2 \ x_3 \ x_4 \ x_5 \ x_6 \ x_7]^T$$

By rewriting equations (1) or (2) into the standard state space form, we have

$$\begin{aligned} \dot{x}(t) &= (M^{-1}A)x(t) + (M^{-1}B)u(t) \\ y(t) &= Cx(t) \end{aligned} \quad (3)$$

which can further be written as

$$\begin{aligned} \dot{x}(t) &= \bar{A}x(t) + \bar{B}u(t) \\ y(t) &= \bar{C}x(t) \end{aligned} \quad (4)$$

where $\bar{A} = M^{-1}A$, $\bar{B} = M^{-1}B$, and $\bar{C} = C$

2.2. Open Loop Nominal Wind Turbine

The nominal values of the *CART2's* state matrices A and B are taken from [22]. The open loop poles obtained from the eigen analysis of matrix A are: $-0.039888 \pm 22.574j$; $-4.4422 \pm 13.508j$; $-0.11715 \pm$

where $x(t)$ is the state vector of length 7, $\dot{x}(t)$ denotes the time derivative of $x(t)$, C represents the output vector to be measured/controlled, M is a 7x7 mass matrix, A is a 7x7 system matrix, B is the control input gain matrix. The rotor collective blade pitch angle, $u(t)$ is considered as the principal control blade pitch angle input, β .

A seven-state linearized wind turbine model considered from [22] is given by equation (2).

The seven states of the system considered in this model are: $x_1(t)$ is the rotor first symmetric flap mode displacement, $x_2(t)$ is the rotor first symmetric flap mode velocity, $x_3(t)$ is the rotor rotational speed, $x_4(t)$ is the drive train torsional spring force, $x_5(t)$ is the generator rotational speed, $x_6(t)$ is the tower first fore-aft mode displacement and $x_7(t)$ is the tower first fore-aft mode velocity. In addition, β represents the rotor collective pitch angle and is the basic control input considered in this paper. The constants M_{ij} , K_{ij} , C_{ij} represents the mass, stiffness and damping elements of the respective matrices ($i, j = 1, 2, \dots, 7$), ζ represents the partial derivative of the rotor aerodynamic torque with respect to β . I_{rot} and I_{gen} represents the moment of inertia of rotor and generator respectively, K_d and C_d represents the stiffness and damping factors.[22]

Table 1. General specifications of the CART2 HAWT Machine.

| Specifications | Type/Numerical Values |
|------------------|-----------------------|
| Turbine type | Horizontal axis |
| | upwind rotor |
| | teetering hub |
| Power regulation | Full span |
| | blade pitch control |
| Number of blades | 2 |
| Rotor speed | 42 rpm |
| Rotor diameter | 43.3m |
| Hub-height | 36.3m |

$5.8673j$ and -0.12094 , which implies there are three pole-pairs and an individual pole. The first and third

pole-pairs are lightly damped and represent the drive-train torsion mode and the tower first fore-aft mode respectively, the second pole-pair represents the rotor first symmetry flap mode which is highly damped whereas the generator speed is represented by the last pole [22]. Speed regulation improves when the generator pole moves farther away to the left from its own open loop value and when damping is increased to the lightly damped pole-pairs. The real part of the first pole is very close to the origin and the slightest of uncertainties in the system parameters will further deteriorate the robust properties which are further discussed in section 3. The general specifications of the wind turbine are given in Table 1.

3. Modelling of Uncertain Wind Turbine

In real time systems, uncertainties are unavoidable, particularly uncertainties are evident in the operation and performance of a wind turbine. Classification of uncertainties may be done based on (i) disturbances due to wind speed variations, noise generated while measurement of the generator speed ω and (ii) dynamic perturbations, that are incurred due to the differences in the mathematical model and the actual dynamics of the wind turbine in operation. Typically the dynamic perturbations include the unmodelled high-frequency dynamics, neglected non-linearities and variations in the system parameters that are due to changes in the environmental conditions, wear-and-tear factors of the wind turbine in operation. The stability and performance of any control system may be adversely affected by these factors.

These dynamic perturbations which occur anywhere in the wind turbine can be lumped into a single block known as the perturbation block or the uncertainty block represented by Δ , as shown in Figure 3. It is called as uncertainty transfer function block $\Delta(s)$. The actual dynamics of the wind turbine model with perturbations $G_{pert}(s)$ (the dotted block in Figure 3) is given by

$$G_{pert}(s) = G_{WT}(s) + \Delta(s) \quad (5)$$

where, $G_{WT}(s)$ is the transfer function of the nominal wind turbine, $\Delta(s)$ corresponds to the parameter variations and is formulated as a diagonal matrix having a certain specified structure [9], therefore it is called "structured uncertainty" represented in the block Δ given by

$$\Delta = \text{diag}[\delta_i a_i] \quad (6)$$

where, $i = 1, 2, 3, \dots, 13$. since, in this analysis there are 13 elements that were chosen to introduce $\pm 25\%$ uncertainty. Uncertainties are caused due to the changes in the values of the elements of the system matrix comprising of mass, damper, spring and inertias of

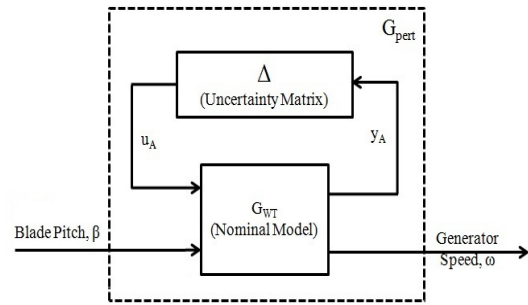


Figure 3. Block diagram representation of an uncertain wind turbine [20].

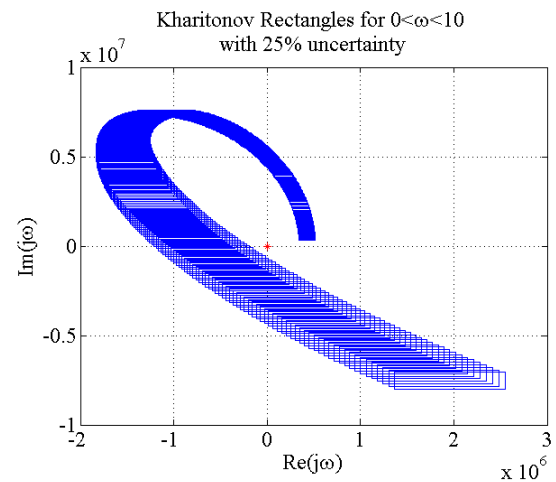


Figure 4. Kharitonov's Rectangles and the zero exclusion principle. Star sign in red color indicates origin.

rotor and generator. In [20], uncertainty was included in 15 elements of the system matrix while in this study, the uncertainties were included in 13 elements to achieve $\pm 25\%$ uncertainty. The nominal system matrix is represented by Equation (3). Here, a_i 's are considered as the system elements of Equation (3) and δ_i are the relative changes in these parameters given by $\delta_i \leq 1$. The perturbed wind turbine with structured uncertainty is represented in a block diagram as shown in figure 3. It is also assumed in this paper that the wind turbine is being operated in the region 2 of the wind speed profile, i.e., from 6 m/s to 11.6 m/s as indicated in [21]. For this range of wind speeds, the blade pitch angle is controlled to regulate the generator speed of a $\pm 25\%$ uncertain CART2 wind turbine.

4. Mathematical Preliminaries of Kharitonov's Theorem Applied to Wind Turbine

Unlike the Routh-Hurwitz stability test that deals with polynomials having fixed coefficients, the Kharitonov's theorem studies the stability of interval polynomials, precisely having uncertain coefficients. The stability of

polynomials are defined in three different ways: firstly, the stability of a polynomial is determined by the left half s-plane roots, secondly, the interval polynomial is said to be robustly stable when all the roots of the given family of polynomials lie in the left half of s-plane and third, when there are restrictions on the settling time, damping factor, etc on the given polynomial or family of polynomials then the concept of D stability is considered where D is a subset of the left half of s-plane and all the roots of the given family of polynomials lie within this sub-region. [11]

Def: *Interval polynomial*: A family of all polynomials is called an interval polynomial given by

$$p(s) = a_0 + a_1s^1 + a_2s^2 + \dots + a_ns^n \quad (7)$$

where $\forall i, a_i \in [l_i, u_i]$ and $0 \notin [l_n, u_n]$.

here, l_i and u_i denotes the minimum and maximum boundary values of the i^{th} coefficient and $0 \notin [l_n, u_n]$ says that all the members of the interval polynomial are of degree n.

There will be four different *Kharitonov's Polynomials* that are formed from the minimum and maximum boundary values [11; 17] given by the following equation

$$p(s, a) = \sum_{i=1}^n [a_i^-, a_i^+] s^i \quad (8)$$

These four fixed polynomials are given by:

$$\begin{aligned} K_1(s) &= a_0^- + a_1^- s^1 + a_2^+ s^2 + a_3^+ s^3 + a_4^- s^4 + a_5^- s^5 + a_6^+ s^6 + \dots \\ K_2(s) &= a_0^+ + a_1^+ s^1 + a_2^- s^2 + a_3^- s^3 + a_4^+ s^4 + a_5^+ s^5 + a_6^- s^6 + \dots \\ K_3(s) &= a_0^+ + a_1^- s^1 + a_2^- s^2 + a_3^+ s^3 + a_4^+ s^4 + a_5^- s^5 + a_6^- s^6 + \dots \\ K_4(s) &= a_0^- + a_1^+ s^1 + a_2^+ s^2 + a_3^- s^3 + a_4^- s^4 + a_5^+ s^5 + a_6^+ s^6 + \dots \end{aligned} \quad (9)$$

Theorem: *Kharitonov's Theorem*: A family of interval polynomial $p(s, a)$ is said to be robustly stable if and only if its four Kharitonov's polynomials are stable. [11]

Lemma: The n^{th} order interval polynomial $p(s, a) = \sum_{i=1}^n [a_i^-, a_i^+] s^i$ is robustly stable if and only if the following is true. [11]

- For $n = 3$, $K_3(s)$ is stable.
- For $n = 4$, $K_2(s)$ and $K_3(s)$ are stable.
- For $n = 5$, $K_2(s)$, $K_3(s)$ and $K_4(s)$ are stable.
- For $n \geq 6$, $K_1(s)$, $K_2(s)$, $K_3(s)$ and $K_4(s)$ are stable.

4.1. Kharitonov's Polynomials of the wind turbine

The transfer function between the output (generator speed, ω) and the control input (blade pitch angle, β)

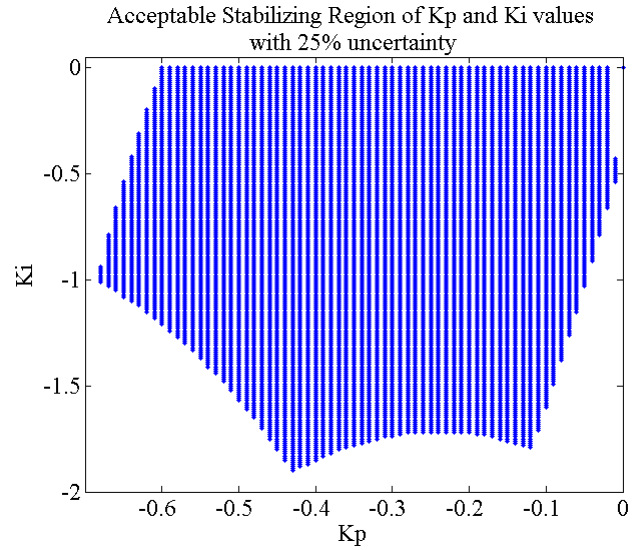


Figure 5. The acceptable stabilizing region when $\pm 25\%$ uncertainty is introduced into the wind turbine model

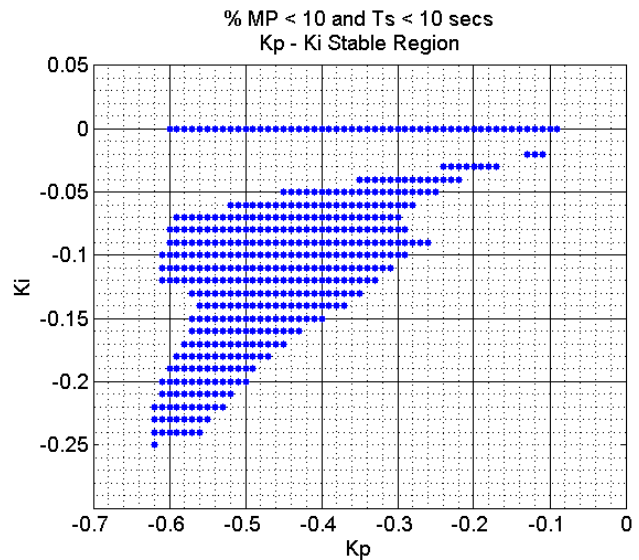


Figure 6. The sub-region of K_p and K_i within the acceptable stabilizing region for $\pm 25\%$ uncertainty to obtain peak overshoot $< 10\%$ and settling time < 10 secs

of the wind turbine is given by the following equation

$$G(s) = \frac{N(s)}{D(s)} \quad (10)$$

where, $N(s)$ and $D(s)$ are the numerator and denominator polynomials of the transfer function of the wind turbine with $\pm 25\%$ uncertainty. Each of the numerator and denominator polynomials yields four Kharitonov's polynomials. The coefficients associated with numerator polynomial and denominator polynomials according to Equation (9) are furnished in Tables 2 and 3 respectively. The nominal, minimum and maximum

values of each of the coefficients for numerator and denominator can be written following the equation (9).

4.2. Kharitonov's Rectangles

For a given family of polynomials represented by equation (9) $p(s, a) = \sum_{i=1}^n [a_i^-, a_i^+] s^i$ rewritten here for convenience. At a given frequency $\omega = \omega_0$, $p(j\omega_0, a)$ which is a set of possible values obtained and the boundaries of the set are given by the four fixed Kharitonov's polynomials $K_1(s)$, $K_2(s)$, $K_3(s)$ and $K_4(s)$. As ω is varied from 0 to ω_0 in small steps, there is a formation of a rectangle for every step variation of ω_0 . If the origin (0,0), lies within these family of rectangles, then the given interval polynomials are unstable, otherwise, it is stable. The family of Kharitonov's rectangles obtained for $\pm 25\%$ uncertainty for the 7-state wind turbine given by equation (2) is shown in Figure 4. Here, according to zero exclusion principle [11], the origin (0,0) is depicted in red color to mark its positioning outside the rectangles .

5. Robust Controller Design using 16-Plant Model

In the design of controller for the interval system having uncertain coefficients in both its numerator and denominator as shown in equation below:

$$p(s, a, b) = \frac{N(s, a)}{D(s, b)} = \frac{\sum_{i=0}^m [a_i^-, a_i^+] s^i}{s^n + \sum_{i=0}^{n-1} [b_i^-, b_i^+] s^i} \quad (11)$$

The assumed equation $p(s, a, b)$ must be a strictly proper. The control scheme is depicted in figure 2

It is required to design a controller $C(s)$ that stabilizes all the members of the interval polynomials belonging to $p(s, a, b)$. There are two different approaches using Kharitonov's theorem: 1. applying kharitonov's theorem to the closed loop denominator and 2. the 16-plant theorem. In this paper, the later method is used wherein Kharitonov polynomials for numerator and denominator are obtained, i.e., $N_1(s)$, $N_2(s)$, $N_3(s)$ and $N_4(s)$ and $D_1(s)$, $D_2(s)$, $D_3(s)$ and $D_4(s)$ are obtained. Hence, there will be 16 Kharitonov plants that are defined by:

$$P_{i_1, i_2} = \frac{N_{i_1}(s)}{D_{i_2}(s)} \quad (12)$$

where $i_1, i_2 \in 1, 2, 3, 4$. The numerator and denominator polynomials are obtained from the coefficients furnished in the Tables 2 and 3 respectively. The nominal, minimum and maximum values of coefficients of the numerator and denominator polynomials are given in Table 2 and Table 3 respectively.

The procedural steps for the design of a suitable controller having acceptable ranges of its parameters

for all the 16-plants obtained from the Kharitonov's theorem:

- The associated 16 plants are calculated from equation (12).
- A first order controller, i.e., a Proportional-Integral (PI) controller given by $C(s) = K_p + \frac{K_i}{s}$ is selected. where, K_p and K_i are the proportional and integral gain constants.
- The Routh-Hurwitz table is utilized to obtain the acceptable ranges of parameters for each member of the 16-plants separately.
- Finally, the intersection of all these 16 inequalities gives the range for acceptable parameters of the controller $C(s)$ that robustly stabilize the given interval plant.

5.1. Acceptable regions for Kp and Ki values of the controller

The wind turbine shown in equation (2) has one input (blade pitch angle, β) and one output (generator speed, ω). The uncertainties in the wind turbine shows deviations in the system response and hence, there is need to design a stabilizing region of Kp and KI to obtain a robust controller. For this, an interval model of the wind turbine is obtained with a $\pm 25\%$ uncertainty, the system matrix of the state space model is given by $M^{-1}A$ in equation 2. The acceptable region for the Kp and Ki values of the proposed PI controller is depicted in Figure 5. It is found that any combination of Kp and Ki in this acceptable region will stabilize the performance of the $\pm 25\%$ uncertain wind turbine, i'e., rated speed of 42 rpm.

Furthermore, a sub-region is provided in Figure 6 which is a part within the acceptable Kp and Ki region is obtained in order to achieve the peak overshoot $< 10\%$ and settling time less than 10 seconds.

In order to analyse the frequency response of the uncertain wind turbine, a region that provides 30° phase margin is obtained and is depicted in Figures 7 and 8.

In Figure 8 the intersection of all 16 inequalities is magnified and shown in the orange shade of the plot that gives the range for acceptable parameters of the controller $C(s)$ to provide 30° phase margin and 11 dB gain margin after robustly stabilizing the given interval plant.

The corner points within the acceptable regions shown in Figures 5, 6 and 7 are selected and plotted for understanding robust stability of the wind turbine in the results section of this paper.

Table 2. Coefficients associated with numerator polynomials.

| Coefficient term | s^4 | s^3 | s^2 | s^1 | s^0 |
|--------------------------|-------|-------|-----------------|----------------|-----------------|
| Nominal, (\bar{a}_i) | 1080 | 5418 | $-2.61 * 10^5$ | $2.073 * 10^5$ | $-1.005 * 10^7$ |
| Min, (\bar{a}_i^-) | 1080 | 3046 | $-2.611 * 10^5$ | $1.105 * 10^5$ | $-1.039 * 10^7$ |
| Max, (\bar{a}_i^+) | 1080 | 5793 | $-2.601 * 10^5$ | $2.203 * 10^5$ | $-1.005 * 10^7$ |

Table 3. Coefficients associated with denominator polynomials.

| Coefficient term | s^7 | s^6 | s^5 | s^4 | s^3 | s^2 | s^1 | s^0 |
|--------------------------|-------|-------|-------|-------|----------------|----------------|----------------|----------------|
| Nominal, (\bar{a}_i) | 1 | 9.314 | 749.8 | 5113 | $1.292 * 10^5$ | $1.977 * 10^5$ | $3.57 * 10^6$ | $4.33 * 10^5$ |
| Min, (\bar{a}_i^-) | 1 | 9.31 | 749.8 | 5092 | $1.289 * 10^5$ | $1.878 * 10^5$ | $3.524 * 10^6$ | $3.426 * 10^5$ |
| Max, (\bar{a}_i^+) | 1 | 9.328 | 750.5 | 5136 | $1.296 * 10^5$ | $2.062 * 10^5$ | $3.623 * 10^6$ | $5.2 * 10^5$ |

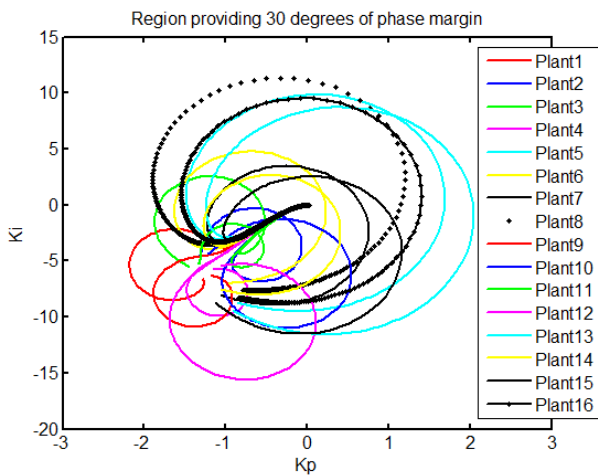


Figure 7. The region that provides robust stability with atleast 30° phase margin within the acceptable stabilizing region when $\pm 25\%$ uncertainty is introduced into the wind turbine model

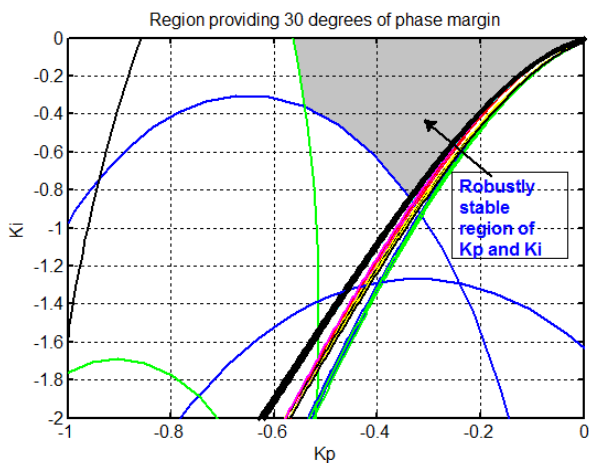


Figure 8. The intersection of all the 16 - Kharitonov plants provides the region of robust stability with atleast 30° phase margin. Magnified view of Figure 7.

6. Results and discussions

After the introduction of uncertainties in the system matrix \bar{A} , a maximum of 150 iterations are simulated to obtain the maximum and minimum values of both numerator and denominator coefficients. A 4th order numerator and a 7th order denominator are formed. The 4 Kharitonov's polynomials for numerator and denominator are obtained separately. The required 16 Kharitonov plants are formed from these 8 (4 each for numerator and denominator) Kharitonov polynomials. The numerator, $N_i(s)$ and denominator, $D_i(s)$ where $i = 1, 2, 3, 4$ for the CART2 HAWT model of the 7-state wind turbine are obtained and are already given in Tables 2 and 3.

In the following subsections, the time and frequency responses of the performance of $\pm 25\%$ uncertain wind turbine are discussed. A few combinations of K_p and K_i are selected from the acceptable regions to study the robust stability. Moreover, the desired time response specifications and frequency response specifications are also discussed.

6.1. Analysis of wind turbine performance in the acceptable K_p and K_i region

In order to analyse the performance of the wind turbine, i.e., the regulation of speed under uncertain conditions of the wind turbine, the following are the combination of values of K_p and K_i considered. They are as follows: (i) $K_{p1} = -0.02$ and $K_{i1} = -0.02$ (ii) $K_{p2} = -0.02$ and $K_{i2} = -0.2$ (iii) $K_{p3} = -0.12$ and $K_{i3} = -0.2$ (iv) $K_{p4} = -0.12$ and $K_{i4} = -1.5$ (v) $K_{p5} = -0.43$ and $K_{i5} = -0.02$ (vi) $K_{p6} = -0.43$ and $K_{i6} = -1.79$ (vii) $K_{p7} = -0.6$ and $K_{i7} = -0.02$ (viii) $K_{p8} = -0.6$ and $K_{i8} = -1.2$.

The simulations of all the 16 plants with these aforementioned eight selected combinations are made to achieve the rated speed 42 rpm of the generator as shown in Figure 9.

The basis for selection of points in the acceptable stabilizing region are as follows: (a) Increasing value of K_p (b) Two different values of K_i for the same value of

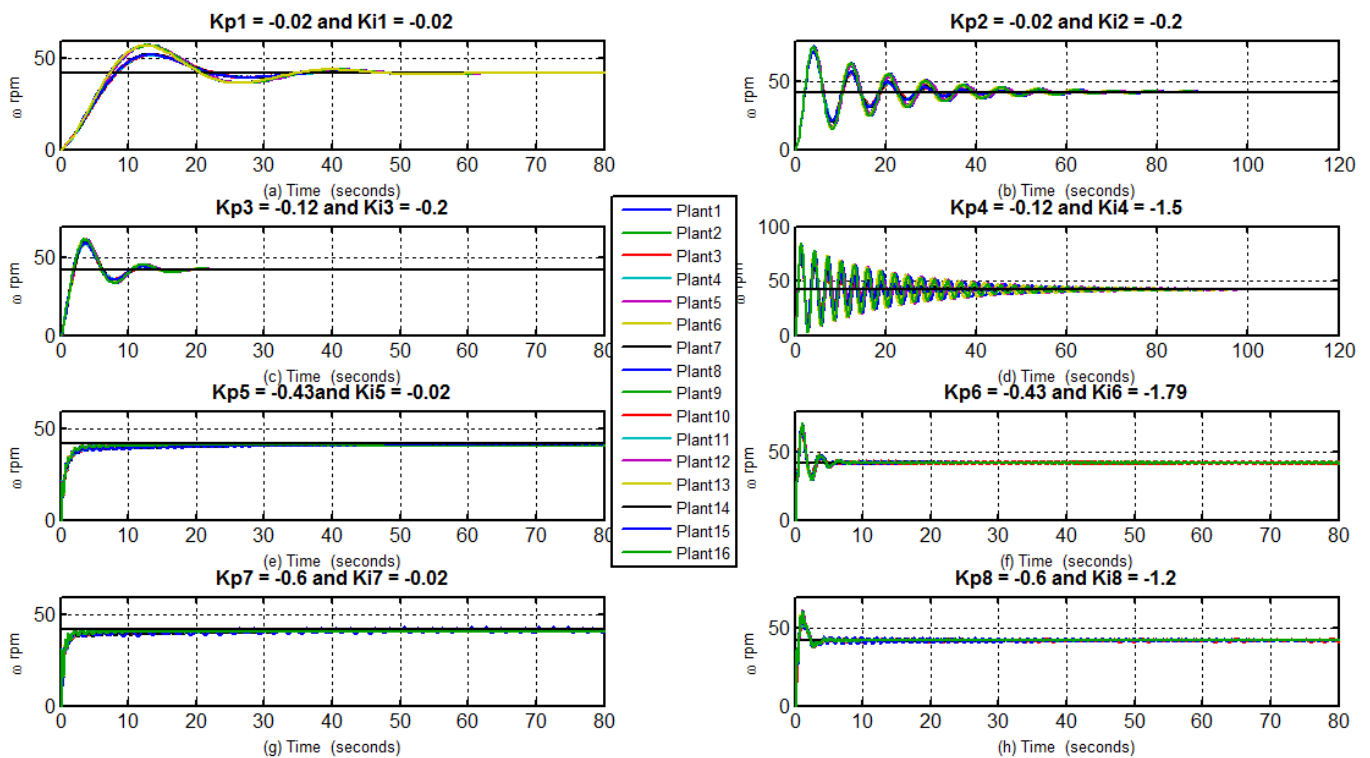


Figure 9. The step responses of 16-Kharitonov plants representing the regulation of speed to 42 rpm by the eight selected points considered for illustration. The points are taken from the K_p and K_i stabilizing region of Figure 5.

K_p (c) The combination of K_p and K_i values selected in the far end of the acceptable stabilizing region of Figure 5.

It is evident from Figure 9 (a and b), that in (a) with $K_p(-0.02)$ and $K_i(-0.02)$ the peak overshoot is less when compared with (b) for higher value of $K_i(-0.2)$. The oscillations are increasing as K_i is increased in the negative direction. Similar oscillations and rise in peak overshoots are visible in the remaining 3 sets of combinations in Figure 9 (c and d), Figure 9 (e and f) and in Figure 9 (f and h). But, eventually it is evident that the effects of $\pm 25\%$ uncertainty are not causing problems in the performance of the uncertain wind turbine, which is regulation of speed to its rated speed of 42 rpm.

Similarly, as K_p is increased in the negative direction, the oscillations and the overshoots for all the 16 Kharitonov’s plants are reduced. Eventually the minimal time response specifications are achieved.

The frequency response analysis is also made for the same sets of K_p and K_i values and are depicted in Figure 10. The plots are depicted for the open loop transfer function to study the closed loop stability of the uncertain wind turbine. The plots are depicted for all the 16 Kharitonov plants.

6.2. Analysis of wind turbine performance in the sub-region of the acceptable K_p and K_i region to achieve the desired time response specifications

In order to achieve a desired peak overshoot of $< 10\%$ and settling time of < 10 seconds after the regulation of speed to rated 42 rpm under uncertain conditions of the wind turbine, the following are the combination of values of K_p and K_i considered from Figure 6. They are as follows: (i) $K_{p1} = -0.11$ and $K_{i1} = -0.02$ (ii) $K_{p2} = -0.2$ and $K_{i2} = -0.03$ (iii) $K_{p3} = -0.3$ and $K_{i3} = -0.1$ (iv) $K_{p4} = -0.4$ and $K_{i4} = -0.14$ (v) $K_{p5} = -0.5$ and $K_{i5} = -0.15$ (vi) $K_{p6} = -0.5$ and $K_{i6} = -0.2$ (vii) $K_{p7} = -0.6$ and $K_{i7} = -0.12$ (viii) $K_{p8} = -0.6$ and $K_{i8} = -0.24$.

The simulations of all the 16 plants with these aforementioned eight selected combinations are made to achieve the rated speed 42 rpm of the generator as shown in Figure 11.

It is evident from Figure 11 (a to h), that for all these values of K_p and K_i , the desired peak overshoot of $< 10\%$ and settling time of < 10 seconds are achieved. The speed is also regulated to the rated 42 rpm under uncertain conditions of the wind turbine. Here again, the effects of $\pm 25\%$ uncertainty are not causing hindrances in the performance of the uncertain wind turbine, which is regulation of speed to its rated speed of 42 rpm.

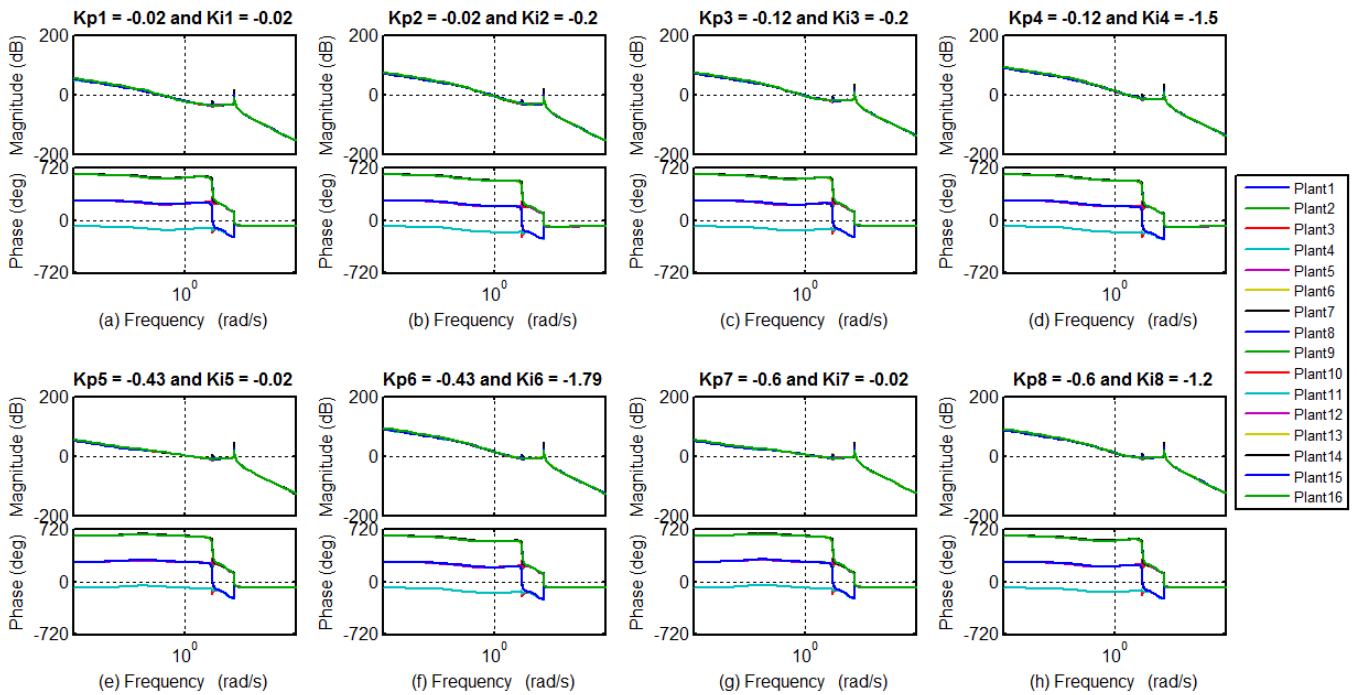


Figure 10. The frequency responses of 16-Kharitonov plants for selected points considered for illustration. The points are taken from the K_p and K_i stabilizing region of Figure 5.

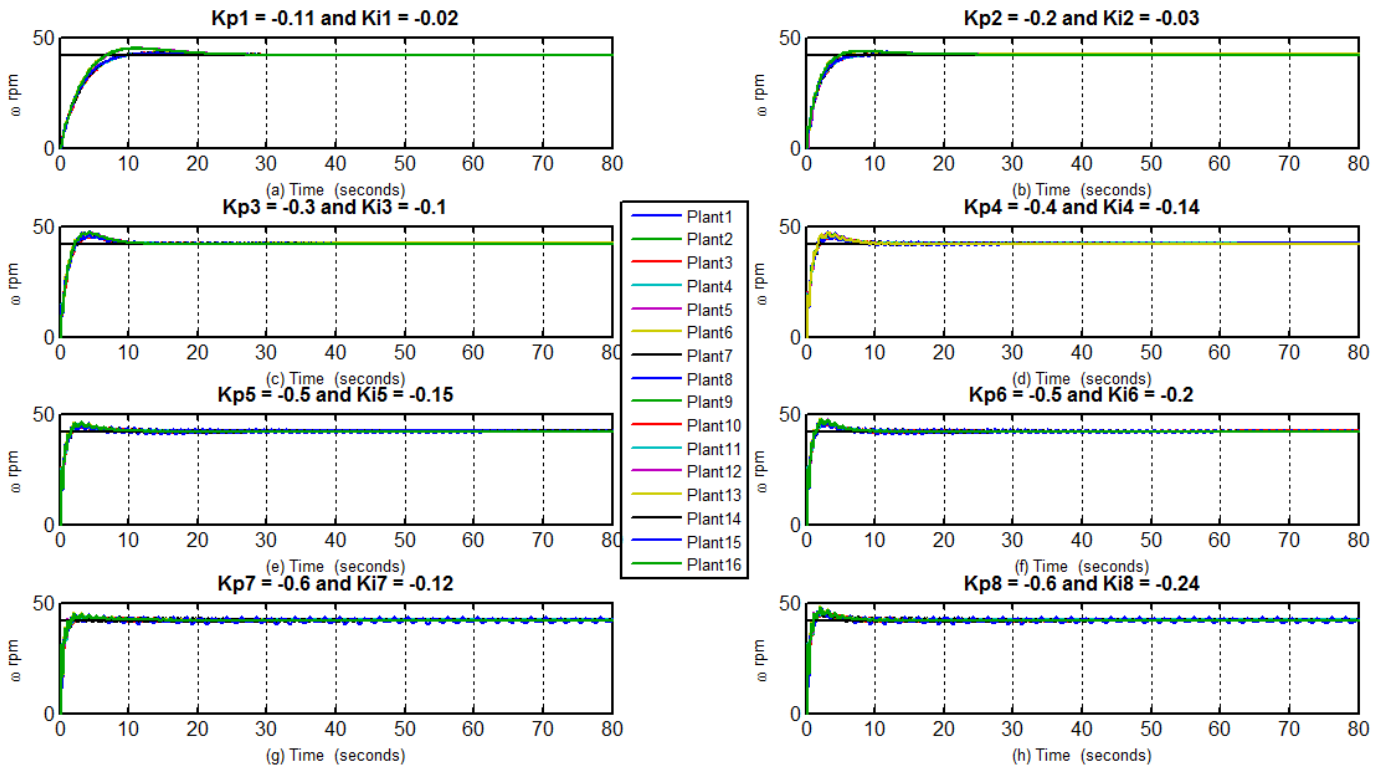


Figure 11. The step responses of 16-Kharitonov plants representing the regulation of speed to 42 rpm with minimal peak overshoot and settling times. The eight selected points are taken from the K_p and K_i stabilizing region of Figure 6

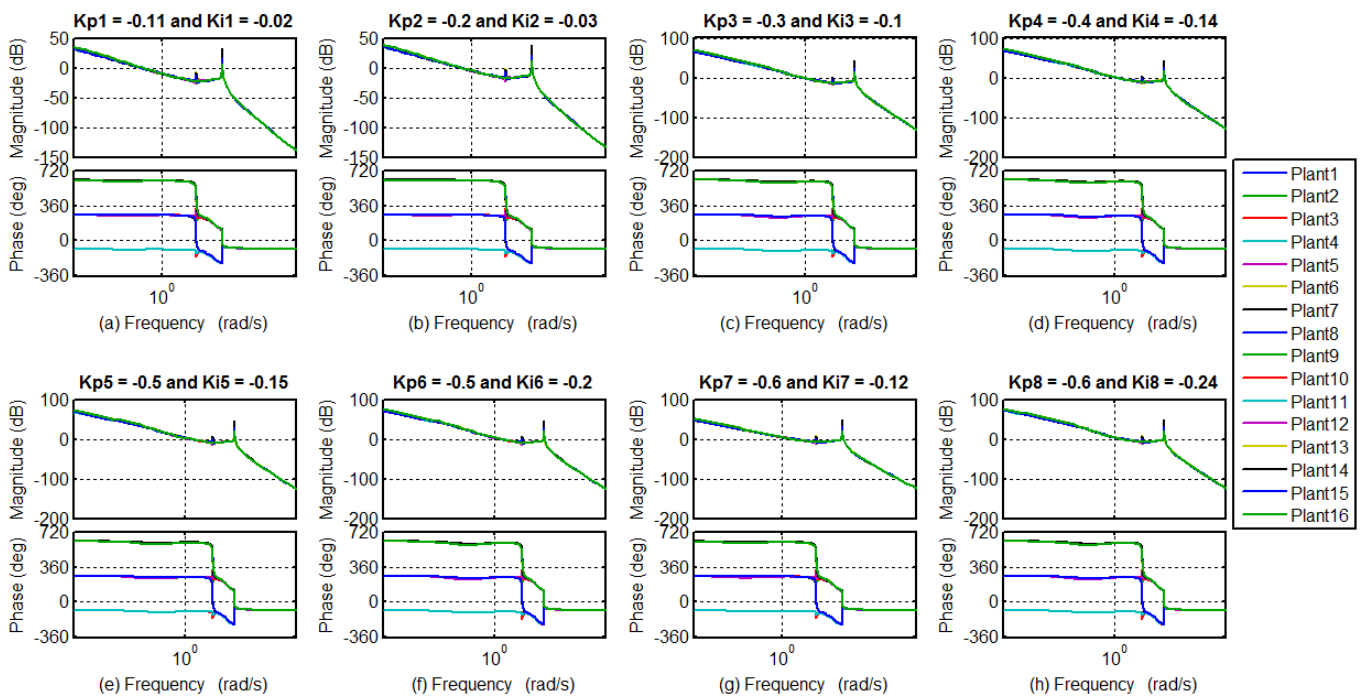


Figure 12. The frequency responses of 16-Kharitonov plants with K_p and K_i values considered from Figure 6. From figures a to h all the 16 Kharitonov plants achieved a minimum of 30° phase margin and atleast 11 dB gain margin.

It is clearly evident from Figure 11 that the oscillations and the overshoots for all the 16 Kharitonov’s plants are reduced. Eventually the minimal time response specifications are achieved.

The frequency response analysis is also made for the same sets of K_p and K_i values and are depicted in Figure 12.

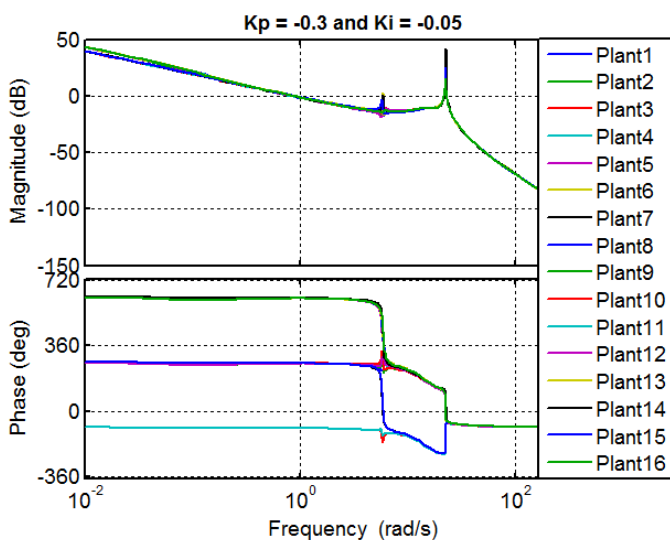


Figure 13. The frequency response plot wherein atleast 30° phase margin is achieved for all 16 Kharitonov plants with $K_p(-0.3)$ and $K_i(-0.7)$ - a point from Figure 8.

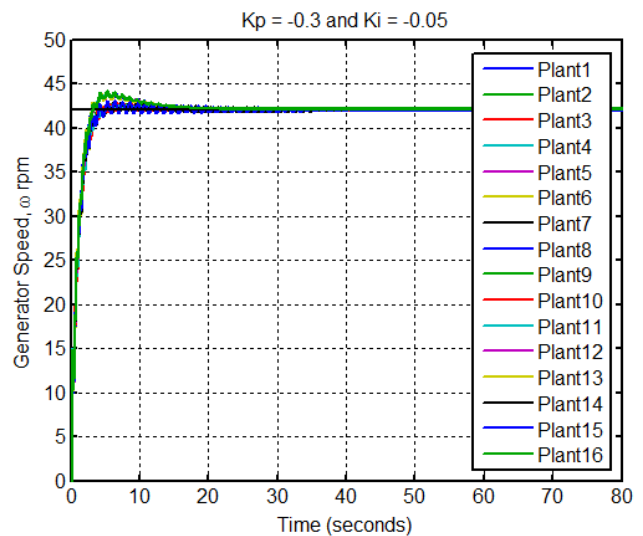


Figure 14. The step response for all 16 Kharitonov plants with $K_p(-0.3)$ and $K_i(-0.7)$.

6.3. Analysis of wind turbine performance in the sub-region of the acceptable K_p and K_i region to achieve the desired frequency response specifications

A controller can be designed to satisfy some performance criterion as well. A certain level of gain and phase margins are considered as the desired gain and phase

margin. In this paper, 30^0 phase margin is desired [11]. As shown in Figures 7 and 8, the K_p and K_i values are considered within the shaded region of Figure 8. The values are -0.3 and -0.05 respectively. A minimum of 30^0 phase margin is achieved for all the 16 Kharitonov plants. Similarly, the frequency response plot for all the 16 plants are shown in Figure 13 to achieve the minimum stability phase margin of 30^0 and gain margin of 11 dB. The step responses of the 16 plants are depicted in Figure 14 wherein the rated speed of 42 rpm is achieved.

7. Conclusion

A robustly stabilizing region of K_p and K_i is proposed by utilizing the Kharitonov theorem based 16-plant interval model for a large scale uncertain wind turbine. The uncertainty in the wind turbine is prominently due to factors like neglecting non-linearities, unmodelled high frequency dynamics, differences in the mathematical model and the actual dynamics and FAST (fatigue, aerodynamics, structural flexibility and wind turbulence). In order to represent these uncertainties a $\pm 25\%$ uncertainty is introduced into the 13 elements of the system matrix of the mathematical model of the wind turbine. This method helps to choose the values of K_p and K_i of a simple PI controller that performs robustly. In this paper, the robust nature of the proposed controller is tested by choosing the robustly stabilizing regions of K_p and K_i in three different ways. Firstly, the acceptable stabilizing region of K_p and K_i for $\pm 25\%$ uncertain wind turbine is obtained. Secondly, the sub-region within the above mentioned region in order to achieve a maximum of 10 % peak overshoot and a maximum settling time of 10 secs is achieved. Lastly, the stabilizing region wherein, at least 30^0 phase margin is achieved by all the 16 Kharitonov plants. The simulated results validated the selection of acceptable stable regions, in order to regulate the speed of the wind turbine to its rated speed of 42 rpm. In this paper, the wind speed is considered to be in the region 2 of the wind profile, this factor is considered for future scope wherein, the authors are in the process of selecting the acceptable regions for wind speed variations acting as external disturbance in their immediate work.

Acknowledgements

The authors express their sincere gratitude to Professor Bharani Chandra Kumar Pakki, Head of the Department of Electrical and Electronics Engineering, GMR Institute of Technology, Rajam, Andhra Pradesh, India.

References

[1] PAO L. Y. and JOHNSON K. E. (2009) *A tutorial on the dynamics and control of wind turbines and wind*

farms. (Paper presented in IEEE American Control Conference), St. Louis, MO, USA, June.

- [2] World Wind Energy Association: (2018) *World wind energy installed capacity*, <https://wwindea.org/blog/2019/02/25/wind-power-capacity-worldwide-reaches-600-gw-539-gw-added-in-2018/>
- [3] LUCY Y. PAO and KATHRYN E. JOHNSON. (2011) *Control of Wind Turbines*. (IEEE Control Systems Magazine), 31 (2): 44–62.
- [4] PAUL A. LYNN. (2011) *Onshore and Offshore Wind Energy: An Introduction*. (UK: John Wiley Sons.)
- [5] BOSSANYI, E. A. (2000) *The Design of Closed Loop Controllers for Wind Turbines*. (Wind energy), 3 (3): 149–163.
- [6] CIVELEK ZAFER, LUY MURAT, CAM ERTUGRUL and BARISCI NECAATTIN. (2016) *Control of Pitch Angle of Wind Turbine by Fuzzy PID Controller*. (Intelligent Automation Soft Computing), 22 (3): 463–471.
- [7] G. RIGATOS and P. SIANO. (2011) *Design of robust electric power system stabilizers using Kharitonov's theorem*. (Mathematics and Computers in Simulation), 82 (): 181–191.
- [8] MING-TZU HO, ANIRUDDHA DATTA and S. P. BHATTACHARYYA (1998) *Design of P, PI and PID Controllers for Interval Plants*. (Proceedings of the American Control Conference), Philadelphia, Pennsylvania June.
- [9] DA-WEI GU, PETKOV H. PETKOV and MIHAIL M. KONSTANTINOV. (2013) *Robust control design with MATLAB®* London: (Springer-Verlag).
- [10] S.P. BHATTACHARYYA. (2017) *Robust control under parametric uncertainty: An overview and recent results*. (Elsevier, Annual Reviews in Control), 44 : 45–77.
- [11] FARZIN ASADI. (2018) *Robust Control of DC-DC Converters The Kharitonov's Theorem Approach with MATLAB Codes*. (A Publication in the Morgan Claypool Publishers series SYNTHESIS LECTURES ON POWER ELECTRONICS Turkey: Morgan & Claypool publishers.)
- [12] S. SWAIN and P.S. KHUNTIA. (2014) *Kharitonov based robust stability for a flight controller*. (International journal of systems signal control and engineering applications), 7 (2): 26–32.
- [13] MOHAMMADREZA TOULABI , AHMAD SALEHI DOBAKSHARI and ALI MOHAMMAD RANJBAR. (2017) *Optimal robust first-order frequency controller design for DFIG-based wind farm utilising 16-plant theorem*. (IET Renewable Power Generation), 12 (3): 298–310.
- [14] RAFIK SALLOUM. (2014) *Robust PID Controller Design for a Real Electromechanical Actuator*. (Acta Polytechnica Hungarica), 11 (5): 125–144.
- [15] MINGHUI CHU and JIZHENG CHU. (2018) *Graphical Robust PID Tuning Based on Uncertain Systems for*

- Disturbance Rejection Satisfying Multiple Objectives.* (International Journal of Control, Automation and Systems), 16 (X): 1–10.
- [16] L.H. KEEL and S.P. BHATTACHARYYA (2016) *Robustness and Fragility of High Order Controllers: A Tutorial.* (IEEE Conference on Control Applications (CCA)), Part of 2016 IEEE Multi-Conference on Systems and Control, Buenos Aires, Argentina, September.
- [17] HAU HUU VO. (2018) *Fast Stability Analysis for Proportional-Integral Controller in Interval Systems.* (Journal of Advanced Engineering and Computation), 2(2): 111–120.
- [18] BIJAN MOAVENI, MOJTABA KHORSHIDI. (2015) *Robust speed controller design for induction motors based on IFOC and Kharitonov theorem.* (Turkish Journal of Electrical Engineering Computer Sciences), 23 (): 1173–1186.
- [19] WANG X., GAO W., GAO T., LI Q., WANG J. and LI X. (2018) *Robust Model Reference Adaptive Control Design for Wind Turbine Speed Regulation Simulated by Using FAST* (Journal of Energy Engineering), 144 (2): 1–12.
- [20] N. V. A. RAVIKUMAR. and G. SARASWATHI. (2019) *Robust controller design for speed regulation of a flexible wind turbine.* (EAI Endorsed Transactions on Energy Web), 6 (23): 1–10.
- [21] NATIONAL RENEWABLE ENERGY LABORATORY. (2004) *Modern control design for flexible wind turbines* (No. NREL/TP-500-35816), National Renewable Energy Lab., Golden, CO (US). 2004.
- [22] ALAN D. WRIGHT and MARK J. BALAS. (2003) *Design of State-Space-Based Control Algorithms for Wind Turbine Speed Regulation.* (Journal of Solar Energy Engineering), 125 (4): 386–395.